Biosci. Rep. (2014) / **34** / art:e00096 / doi 10.1042/BSR20130135

OPEN ACCESS

Original Paper

Bioscience Reports

www.bioscirep.org

Bioscience Reports

A new glycation product 'norpronyl-lysine,' and direct characterization of cross linking and other glycation adducts: NMR of model compounds and collagen

Peter T. B. BULLOCK*, David G. REID*, W. YING CHOW*, Wendy P. W. LAU* and Melinda J. DUER*[1]

*Department of Chemistry, University of Cambridge, Lensfield Road, Cambridge CB2 1EW, U.K.

Synopsis

NMR is ideal for characterizing non-enzymatic protein glycation, including AGEs (advanced glycation endproducts) underlying tissue pathologies in diabetes and ageing. Ribose, R5P (ribose-5-phosphate) and ADPR (ADP-ribose), could be significant and underinvestigated biological glycating agents especially in chronic inflammation. Using [U-^{13}C]ribose we have identified a novel glycoxidation adduct, 5-deoxy-5-desmethylpronyl-lysine, 'norpronyl-lysine', as well as numerous free ketones, acids and amino group reaction products. Glycation by R5P and ADPR proceeds rapidly with R5P generating a brown precipitate with PLL (poly-L-lysine) within hours. ssNMR (solid-state NMR) ^{13}C–^{13}C COSY identifies several crosslinking adducts such as the newly identified norpronyl-lysine, *in situ*, from the glycating reaction of $^{13}C_5$-ribose with collagen. The same adducts are also identifiable after reaction of collagen with R5P. We also demonstrate for the first time bio-amine (spermidine, N-acetyl lysine, PLL) catalysed ribose 2-epimerization to arabinose at physiological pH. This work raises the prospect of advancing understanding of the mechanisms and consequences of glycation in actual tissues, *in vitro* or even *ex vivo*, using NMR isotope-labelled glycating agents, without analyses requiring chemical or enzymatic degradations, or prior assumptions about glycation products.

Key words: ADP-ribose, advanced glycation endproducts, Maillard reaction, ribose, ribose-5-phosphate, solid-state NMR

Cite this article as: Bullock, P. T. B., Reid, D. G., Ying Chow, W., Lau, W. P. W. and Duer, M. J. (2014) A new glycation product 'norpronyl-lysine,' and direct characterization of cross linking and other glycation adducts: NMR of model compounds and collagen. Biosci. Rep. **34**(2), art:e00096.doi:10.1042/BSR20130135

INTRODUCTION

Glycation (non-enzymatic glycosylation) is the reaction of sugars to form covalent adducts with proteins. It occurs wherever sugars and proteins are in contact, usually initially through so-called Maillard reactions (see Supplementary Data Section S1; available at http://www.bioscirep.org/bsr/034/bsr034e096add.htm for summaries of these, and other glycation reactions and products and their abbreviations). Initial products react further to form AGEs (advanced glycation endproducts), including protein modifications, sugar degradation products and protein crosslinks, the latter implicated in numerous conditions including diabetes, atherosclerosis, osteoarthritis and cataracts [1,2]. The Maillard reaction with glucose *in vivo* is slow at physiological temperature and pH due to its low reactivity, so only long-lived structural proteins such as collagen and elastin are significantly affected by crosslinking arising from glycation by this sugar [2].

Collagen crosslinking is a poorly understood pathological consequence of glycation, leading to irreversible degeneration of mechanical properties, such as stiffer, more brittle connective tissue fibres. Both crosslinking and simple modifications of amino acid side-chains can lead to abnormal biochemical functionality of collagen by changing the charge profile of the collagen fibrils, with unpredictable consequences [3]. For instance, modification of lysine residues to the relatively

Abbreviations: ADPR, ADP-ribose; AGE, advanced glycation endproduct; CEL, carboxyethyl lysine; CML, carboxymethyl lysine; CP, cross polarization; DOPDIC, N6-{2-{[(4S)-4-ammonio-5-oxido-5-oxopentyl]amino}-5-[(2S)-2,3-ydihydroxypropyl]-3,5-dihydro-4H-imidazol-4-ylidene}-L-lysinate; GOLD, glyoxal lysine dimer; MOLD, methylglyoxal lysine dimer; PAR, poly-ADP-ribose; PLL, poly-L-lysine; POST-C7, permutationally offset stabilized C7; R5P, ribose-5-phosphate; SQ–DQ, single quantum–double quantum; ssNMR, solid-state NMR.

[1] To whom correspondence should be addressed (email mjd13@cam.ac.uk).

© 2014 The Author(s) This is an Open Access article distributed under the terms of the Creative Commons Attribution Licence (CC-BY) (http://creativecommons.org/licenses/by/3.0/) which permits unrestricted use, distribution and reproduction in any medium, provided the original work is properly cited.

common AGEs N^{ε}-CML [(carboxymethyl)lysine] and N^{ε}-CEL [(carboxyethyl)lysine] changes a positively charged into a negatively charged side-chain.

Research has focused on glycation by glucose, assumed to be the most relevant sugar in both non-pathological tissues and hyperglycaemic conditions. However, glucose is not an efficient glycating agent as it overwhelmingly adopts its thermodynamically stable pyranose form, rather than the reactive open-chain aldehyde form. Pentoses such as ribose and especially R5P (ribose-5-phosphate) are much more potent glycating agents, R5P reacting with amines 150-fold faster than glucose [4,5]. R5P and the mechanistically almost indistinguishable ADPR (adenosine diphosphate ribose) are both released into the extra-cellular matrix on cell necrosis, so are present in chronic inflammation where there is long-term cellular damage, and so could be potent biologically significant and, to date, under-investigated glycating agents. Some established reaction pathways to AGEs are not available to R5P or ADPR due to phosphoesterification of the terminal ribosyl 5-carbon; equally, it is possible that there are glycation products of R5P or ADPR that do not occur for glucose. The aim of this work is to identify the possible glycation products of ribose, R5P and ADPR in both model systems and collagen itself.

Glycation products can be detected by a variety of techniques in different tissues and experimental models systems [6–20], including solution state NMR (hereafter simply referred to as 'NMR' in distinction to ssNMR (solid-state NMR)), which can detect soluble AGEs [12,21–23]. Although all these previous approaches yield valuable chemical and mechanistic insights, they are only applicable with considerable prior sample preparation to the large insoluble structural proteins, which are significant pathogenic targets of tissue glycation. ssNMR, however, bypasses many of these difficulties and can access a wealth of chemical information from these solid materials in a close to native state. Thus, in this work we develop NMR spectroscopic and labelling approaches to analysing mixtures of glycation products, in particular those from ribose, R5P and ADPR, and to exploring the products of glycation of collagen itself. The approaches we develop could find applications in the study of tissue glycation in hyperglycaemic diseases such as diabetes.

MATERIALS AND METHODS

Reagents were from Sigma–Aldrich except [U-^{13}C]ribose, which was from Cambridge Isotope Laboratories. PLL (poly-L-lysine) hydrobromide was molecular mass 4,000–15,000 Da. Reagent salt forms were: Spermidine trihydrochloride, disodium R5P, sodium ADPR. Dry Type I collagen (bovine Achilles tendon) was rehydrated by soaking overnight in aqueous acetic acid (10 %), homogenized with a hand held plunger homogenizer, and washed with distilled water and centrifuged repetitively until no longer acidic, and stored wet at 4 °C until used. All incubations were performed at 37 °C in 50 mM potassium phosphate at pH 7.4 in 5 % D_2O/H_2O to which a few crystals of sodium azide had been added to ensure sterility, unless otherwise indicated, and progress was monitored periodically by NMR. Glycation products were shown to be reproducible by repeating each experiment.

Glycation of model amines

Composition of individual reaction mixtures in 1.05 ml (unless stated otherwise) solution are summarized below. To facilitate periodic analyses by NMR these reactions were performed in 4 mm outer diameter glass NMR tubes.

α-N-acetyl lysine

AcLys 9.5 mg, ribose 7.5 mg; AcLys 9.5 mg, [U-^{13}C]ribose 7.5 mg; AcLys 9.5 mg R5P 13 mg.

Spermidine

Spermidine 13 mg, ribose 7.5 mg; Spermidine 13 mg, R5P 13 mg.

PLL

PLL 12 mg, ribose 7.5 mg; PLL 12 mg, [U-^{13}C]ribose 7.5 mg; PLL 12 mg, ADPR 28 mg.

Controls

Ribose (7.5 mg), [U-^{13}C]ribose (7.5 mg), and R5P (12 mg), were each incubated for a month; the spectrum of each was unchanged after this time.

Glycation of samples for ssNMR

Large scale glycation of PLL

550 mg PLL and 750 mg R5P were incubated in 45 cm^3 buffer containing sodium azide for a day. The resultant brown precipitate was washed with 40 ml water and centrifuged, three times, and air dried overnight for ssNMR.

Collagen incubations under biomimetic conditions

2 g wet mass of collagen was used in all incubations. A few crystals of sodium azide were added to incubations for sterility. All glycated solids were washed with 40 ml water and centrifuged, three times, and air dried overnight for ssNMR.

Collagen and R5P: a mixture of collagen and 60 mg R5P disodium salt was made up to 4 cm^3 with water and incubated at 310 K for 14 days. Phosphate buffer (1 M, 2 ml) was added after 8 days. The glycated collagen was distinctly yellow at this point.

Collagen and [U-^{13}C]ribose: a mixture of collagen and [U-^{13}C]ribose (35 mg) was made up to 4 cm^3 with phosphate buffer (50 mM) and incubated for 69 days, at which point the collagen was distinctly orange. The pale yellow supernatant was collected for NMR analysis.

Collagen and R5P (pH 9, sonicated): a mixture of collagen (2 g, wet) and R5P (60 mg) was made up to 4 cm^3 with phosphate buffer (100 mM, pH 9.0 attained with NaOH), sonicated

© 2014 The Author(s) This is an Open Access article distributed under the terms of the Creative Commons Attribution Licence (CC-BY) (http://creativecommons.org/licenses/by/3.0/) which permits unrestricted use, distribution and reproduction in any medium, provided the original work is properly cited.

and incubated at 310 K for 11 days, at which point the collagen was yellow.

NMR

All ^{13}C and ^{31}P experiments were performed in $H_2O/^2H_2O$ using standard methodology on a Bruker 11.8 Tesla Avance-500 standard bore spectrometer, at frequencies of 500.1 MHz (^1H), 125.6 MHz (^{13}C) and 202 MHz (^{31}P). Pulse-acquire and ^{13}C-^{13}C COSY, was performed with continuous broadband decoupling. ^{13}C and ^{31}P chemical shifts were referenced, respectively, to internal TSP (trimethylsilapentane) sulfonate sodium salt, and external 85% phosphoric acid, at 0 ppm.

ssNMR

All measurements were performed on a Bruker 9.4 T Avance-400 wide bore spectrometer, with a standard Bruker MAS 4 mm double resonance probe operating at 400.4 MHz, 100.6 MHz and 162.1 MHz for ^1H, ^{13}C and ^{31}P, respectively. Samples were in 4 mm zirconia rotors and spun at 12.5 kHz at the 'magic' angle of 54.7° unless stated otherwise. CP (cross-polarization) from ^1H was used to enhance signal intensity (^1H $\pi/2$ pulse 2.5 μs, CP field strength 70 kHz, CP time 2.5 ms, spinal64 broadband decoupling (100 kHz field) during acquisition, repetition time 2 s. SQ–DQ (single quantum–double quantum) ^{13}C-^{13}C ssNMR correlation was achieved using POST-C7 (permutationally offset stabilized C7) [24] methodology and MAS (magic angle spinning) frequency of 10 kHz. ^{13}C and ^{31}P spectra were referenced to the glycine Cα signal at 43.1 ppm, and to hydroxyapatite at 2.6 ppm, respectively.

RESULTS

Many protein gyrations occur through lysyl amines, so in this work these processes were modelled by using the simpler amines PLL, AcLys and spermidine as models before examining the glycation of collagen. Glycation reactions with ribose, R5P and ADPR all produced numerous AGEs and AGE analogues, which we categorize as (i) sugar modifications, (ii) protein side chain modifications and (iii) cross links.

Sugar modifications

The majority of Maillard reactions do not in fact consume the amine [5], rather the amine catalyses sugar degradations and rearrangements, which would not occur in the absence of amines.

Catalytic epimerization of ribose

All the amines catalyse epimerization of ribose into arabinose, readily shown by the replacement of ribose NMR signals by signals characteristic [25] of the two anomeric forms of arabinose as the reactions proceed (Supplementary Data Section S2 Figure S2; available at http://www.bioscirep.org/bsr/034/bsr034e096add.htm). This result is significant because, although previously observed in strong alkali [26], such rearrangements have not been reported before in such mild biomimetic conditions as those used in this work. This suggests that the amine is integral to the mechanism of epimerization, with the reaction mechanism in Supplementary Data Section S1 Scheme 1 explaining the observation if the Amadori rearrangement (Step 2) is significantly reversible.

Generation of carboxylic acids

Simple carboxylic acids were common Maillard products detected in all reaction systems. Supplementary Data Section S3 Table S1 (available at http://www.bioscirep.org/bsr/034/bsr034e096add.htm) summarizes likely assignment of ^{13}C solution-state NMR signals from possible 1- and 2-carbon atom acids resulting from oxidative degradation of ribose and R5P. Formic, acetic and glycolic acids were abundant AGEs from all reaction mixtures, with oxalic acid also common although generated in smaller quantities; the occurrences of these acids is summarized in Supplementary Data Section 3 Table S2. Acetic and glycolic acids are unlikely to have any pathological effects, formic acid is metabolized rapidly, but even so its generation by glycation in the eyes may have pathological consequences due to its high ocular toxicity. Oxalic acid generation in sufficient concentrations may lead to pathological precipitation of calcium oxalate, the most significant component of kidney stones.

Norfuraneol

This was observed in all ribose/amine incubations, but not in R5P/amine incubations. A full ^{13}C solution-state NMR assignment of ^{13}C norfuraneol is given in Supplementary Data Section S4 Table S3 (available at http://www.bioscirep.org/bsr/034/bsr034e096add.htm). The lack of norfuraneol as an AGE in reactions of R5P was expected [5] as R5P lacks the C5 hydroxyl group necessary for the final cyclization step that produces norfuraneol (see Online Supplemental Material Scheme S2).

Protein side chain modifications

Amadori compound

All incubations of ribose or R5P with amines yielded a small transient ^{13}C NMR signal at 208–210 ppm (Online Supplementary Material Section S5; available at http://www.bioscirep.org/bsr/034/bsr034e096add.htm), most likely due to the Amadori product, ribuloselysine (or 5-phospho-ribuloselysine, see Supplementary Data Scheme S1), which is predicted to be present at low concentrations according to steady-state kinetics. The signal appears as a doublet of doublets (J = 46 and 40 Hz) in the $^{13}C_5$-ribose/AcLys system, and shows ^{13}C-^{13}C COSY correlations to signals at 57 and 79 ppm in the $^{13}C_5$-ribose/PLL system, as expected for the ribuloselysine carbonyl carbon [27]. This suggests that the progress of the Maillard reaction *in vitro*

© 2014 The Author(s) This is an Open Access article distributed under the terms of the Creative Commons Attribution Licence (CC-BY) (http://creativecommons.org/licenses/by/3.0/) which permits unrestricted use, distribution and reproduction in any medium, provided the original work is properly cited.

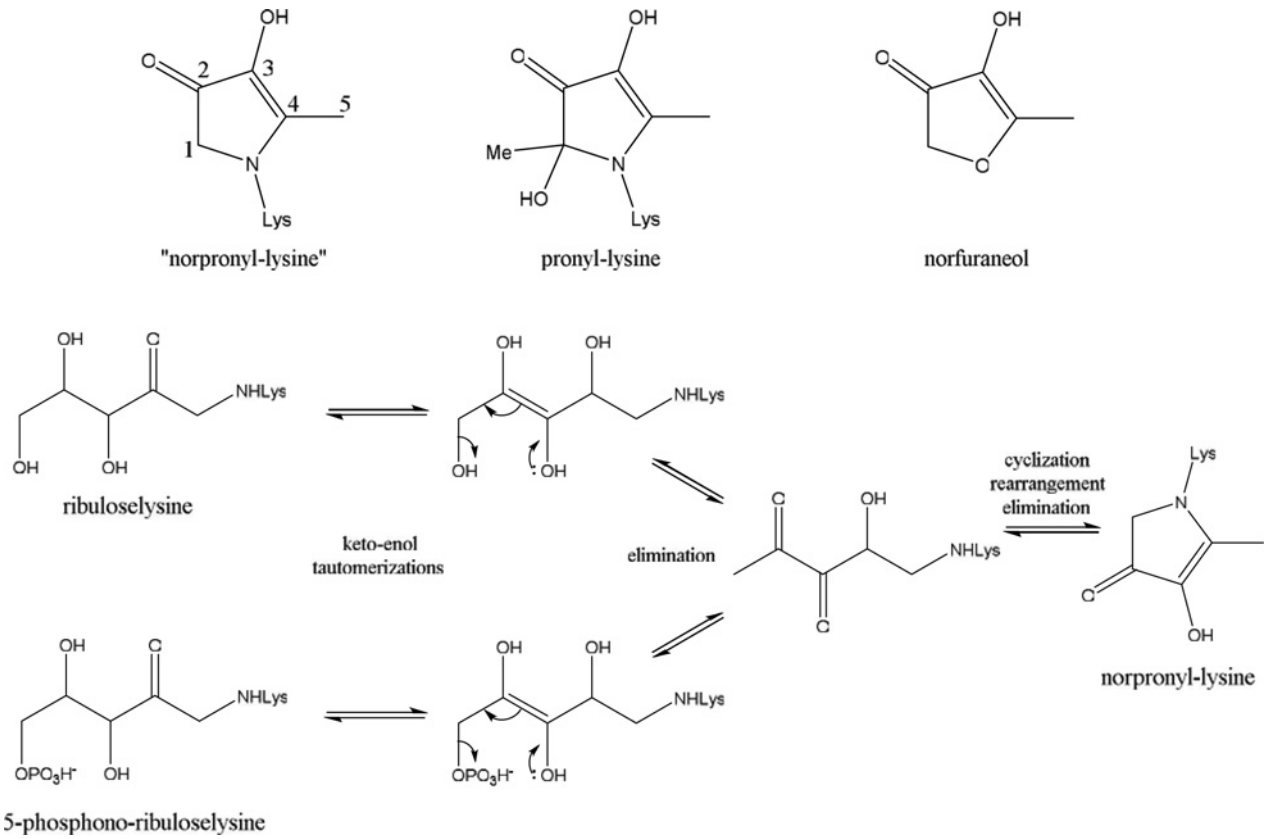

Scheme 1 **Postulated mechanism of formation of norpronyl-lysine from the Amadori products of both ribose and R5P with lysine**
Note the similarity to the established mechanism of formation of norfuraneol in the cyclization, rearrangement and elimination of water (Online Supplemental Material Section S1 Scheme S2).

can be monitored by the evolution of this ca. 209 ppm signal, since once it has disappeared, the initial glycation step (whereby free ribose becomes covalently bound to the amine) must be complete.

CML and CEL

The anticipated AGE, CML, was readily identified by ^{13}C NMR spectroscopy as a pair of signals at 52.1 and 174.3 ppm (^{13}C-enriched ribose experiments yielded two doublets, $J = 53$ Hz). In the liquid state this provides a very straightforward diagnostic for CML. However, since in a protein the peptide α-carbons and carbonyls resonate at ~50 and ~175 ppm, respectively, in the solid state there is no chance of resolving CML signals from those of the protein without selective ^{13}C enrichment. No evidence was found for CEL as a glycation product with ribose, R5P or ADPR; since the methyl carbon of CEL gives a distinctive resonance at ~15 ppm [28], the absence of such a signal implies that very little CEL was generated.

Acetylation

^{13}C-^{13}C COSY analysis of $^{13}C_5$-ribosylated PLL reveals a correlation between 23 and 177 ppm. This is characteristic of an acetyl amide, N^{ε}-acetyl lysine, a known AGE.

Discovery of a novel pyrrolinone reductone AGE

A set of five COSY correlated ^{13}C resonances were well resolved in [U-^{13}C]ribosylated PLL (Figure 1) and in [U-^{13}C]ribosylated AcLys, at 59 ↔ 187 ↔ 130 ↔ 176 ↔ 14 ppm due to a previously unreported pyrrolinone reductone [29] AGE for which we propose the name 'norpronyl-lysine' for its similarity to the established AGE pronyl-lysine [30]. A full assignment of the ^{13}C NMR spectrum of norpronyl-lysine including through-bond coupling constants (J_{CC} values) is given in Table 1.

Norpronyl-lysine is postulated to form by 5-elimination from the Amadori product [31] followed by cyclization, rearrangement and dehydration (Scheme 1). This mechanism implies that R5P should undergo conversion to norpronyl-lysine more readily than ribose as elimination of a phosphate group proceeds

© 2014 The Author(s) This is an Open Access article distributed under the terms of the Creative Commons Attribution Licence (CC-BY) (http://creativecommons.org/licenses/by/3.0/) which permits unrestricted use, distribution and reproduction in any medium, provided the original work is properly cited.

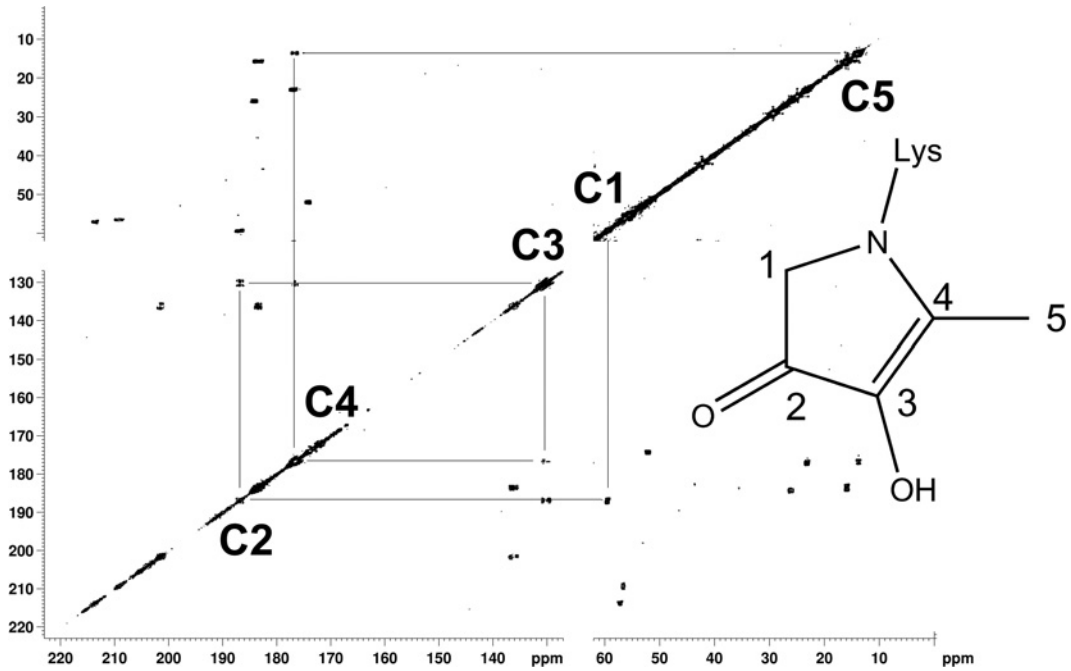

Figure 1 **^{13}C–^{13}C COSY correlation spectrum of [U-^{13}C]ribose glycated PLL**
Portions of the 2D ^{13}C-^{13}C COSY correlation spectrum acquired from PLL after 10 days incubation with $^{13}C_5$-ribose. The data is presented as a contour plot in which the diagonal (bottom left to top right) represents a conventional 1D spectrum 'viewed from above'. The off-diagonal 'cross peak' features connect signals between carbon atoms which are directly bonded to each other, at chemical shifts (i.e. frequencies) which are effectively Cartesian coordinates of the two bonded atoms. Cross peaks corresponding to the norpronyl group (shown) are assigned and connected by solid vertical and horizontal lines.

Table 1 Full assignment of $^{13}C_5$-norpronyl-lysine as observed after glycation of AcLys by [U-^{13}C]ribose

carbon atom	Δ (ppm)	Multiplicity	*J* (Hz)
1	59.3	dd	43, 19
2	186.6	ddd	73, 43, 14
3	129.9	ddd	77, 73, 19
4	176.6	ddd	77, 44, 14
5	13.6	d	44

preferably to elimination of hydroxide, and we do indeed observe norpronyl-lysine in the incubations of R5P with PLL and collagen (see later). In a similar experiment studying the reaction between R5P and AcLys in non-oxidative conditions, a compound by LC/MS of mass equivalent to [AcLys-NH_2 + 96] was reported with no firm assignment [5], consistent with the generation of norpronyl-lysine, though unrecognized at the time. Reaction of PLL with R5P and ADPR results in rapid formation of a brown solid (see following section for more detailed discussion of the AGEs arising from these reactions) and thus we have to use ssNMR to assess the products from these glycation reactions. Amongst the many product signals (see following section) is one at 192 ppm, an unusual ^{13}C chemical shift, higher in frequency than an acid, ester or amide but lower than a ketone, not reported before in glycation reactions with pentose sugars. By comparison with the ribose/PLL system it appears to be due to norpronyl-lysine. The change in chemical shift of the carbonyl group between liquid state and solid state (~5 ppm) is not unexpected, and is attributable to packing effects in solids which are not operative in the liquid, and/or changes in hydrogen bonding between solid and solution state.

The biological effects of norpronyl-lysine can only be speculated at, but the very similar lysine modification pronyl-lysine may be a free radical scavenging antioxidant which inhibits development of colonic precancerous lesions [32]. On the other hand, as a protein modification it is likely to have a negative impact on the functionality of collagen and on collagen recycling by collagenases.

Crosslinking

PLL with R5P, and with ADPR

Reaction between R5P and PLL led to precipitation of a brown polymer after only a few hours, attributed to the formation of crosslinks between the strands of PLL. This dramatic glycation effect was also observed for ADPR and shown, by ^{31}P and ^{13}C NMR (Supplementary Data Section S6 Figures S4 and S5; available at http://www.biosciprep.org/bsr/034/bsr034e096add.htm, respectively), to proceed *via* elimination of ADP, consistent with the literature [5] and further corroborated by ^{31}P ssNMR

© 2014 The Author(s) This is an Open Access article distributed under the terms of the Creative Commons Attribution Licence (CC-BY) (http://creativecommons.org/licenses/by/3.0/) which permits unrestricted use, distribution and reproduction in any medium, provided the original work is properly cited.

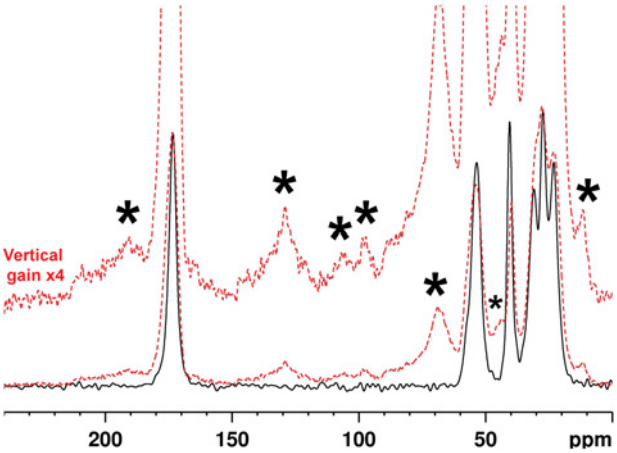

Figure 2 ^{13}C ssNMR from the PLL–R5P reaction

^{13}C ssNMR of PLL before (black solid lines, bottom) and after (red, dashed lines) incubation with R5P Glycation broadens the PLL peaks due probably to increased chemical diversity. The most significant new signals characterized by signal-to-noise ratios of greater than 5, are asterisked. Tentative assignments are: 130 and 10 ppm–MOLD; 130 ppm could indicate some GOLD; 70 ppm–secondary alcohol resonances from intact sugars or sugar degradation products bound into the polymer, and/or lysyl modifications such as N^{ε}-glyceryl lysine; 44 ppm could correspond to C_{ε} of a modified lysine such as MOLD (which would explain the broadness as many modifications are possible). 192 ppm is from norpronyl-lysine. See Online Supplemental Material Section S1 Figure S1 for chemical structures of glycation products.

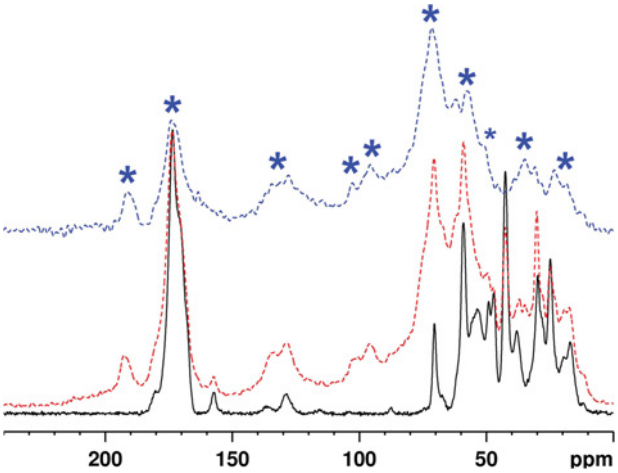

Figure 3 ^{13}C ssNMR of the collagen-[U-^{13}C]ribose reaction

^{13}C ssNMR spectrum of $^{13}C_5$-ribosylated collagen (69 days incubation, red, dashed middle trace), and ^{13}C 1D SQ–DQ spectrum 'filtered' using the POST-C7 technique (blue, dashed upper trace), shown relative to unglycated collagen incubated for the same period (black, lower trace). Resolved new signals derived from the ribose are marked with asterisks, but there are broad areas of new signal throughout the range 10–215 ppm as is evident from the 1D SQ–DQ filtered spectrum, which shows only signals from ^{13}C directly bound to another ^{13}C and hence unambiguously derived from [U-^{13}C]ribose.

(Supplementary Data Section S6 Figure S6). Glycation of PLL by R5P led to generation of reaction products with ^{13}C ssNMR signals consistent with the expected crosslinks MOLD (methylglyoxal lysine dimer) [33] and GOLD (glyoxal lysine dimmer) [34], with the resonance at 10 ppm particularly diagnostic of MOLD, as well as signal in the sugar region (60–80 ppm) from several overlapping components (Figure 2) consistent with both of these species.

Glycation of collagen

Reactions with [U-13C]ribose

Incubation of collagen with [U-^{13}C]ribose led to numerous reaction products derived from the ribose, whose NMR signals could be separated from those of the unaltered collagen components using double-quantum filtering in the NMR experiment (the 1D POST-C7 experiment; Figure 3). This procedure removes all signals from ^{13}C atoms not directly bonded to another ^{13}C so effectively only shows those which originate from [U-^{13}C]ribose. Assignment was aided by 2D SQ–DQ correlations between covalently bonded ^{13}C pairs (Figure 4), which demonstrated that many signals are superpositions of signals from two or more AGEs.

The most intense signal in the ^{13}C-^{13}C SQ–DQ spectrum is from secondary alcohols at 65–75 ppm, such as the Amadori product ribuloselysine and certain AGEs such as DOPDIC (N6-{2-{[(4S)-4-ammonio-5-oxido-5-oxopentyl]amino}-5-[(2S)-2,3-ydihydroxypropyl]-3,5-dihydro-4H-imidazol-4-ylidene}-L-lysinate) and glyceric acid. The strong correlation between 35 and 59 ppm is evidence for pentosinane and/or its hydrolysis product DOPDIC [11]. Correlations between 55 and 175 ppm are consistent with AGEs which share the imidazole lysine-arginine crosslink motif (Figure 4), the closely related pentosinane, and CML and CEL. The correlation between 17 and 57 ppm corresponds to a methyl group adjacent to an amine, functionalized to give in turn a correlation between 23 and 174 ppm, characteristic of an acetyl group in an acid, ester or amide. It is probably due to N^{ε}-acetyl lysine, as the alternative, an ester, has never been reported as a stable AGE. The correlation between 59 and 192 ppm cannot be explained by any of the established AGEs, but is entirely consistent with the newly characterized norpronyl-lysine. The weakest correlation between 56 and 102 ppm corresponds to the furanose form of ribuloselysine [27]. Its persistence after 69 days of reaction suggests the Amadori product is more stable in the solid state than in solution. NMR spectral assignments thus far are summarized in Table 2. (Two autocorrelations, of the 31 ppm, and the 88 ppm, signals to themselves or other atoms with very similar shifts, have not yet been assigned.)

^{13}C NMR of the supernatant at the end of the incubation showed a variety of soluble AGEs, including large quantities of glycolic and oxalic acids (Supplementary Data Section S7 Figure S7, http://www.bioscirep.org/bsr/034/bsr034e096add.htm). In addition there were many new signals that did not correspond to anything seen in any of the model systems, particularly several signals between 20 and 40 ppm (Supplementary Data Section S7 Figure S8). Signals due to CML were observed, which suggests that some protein or amino acids have been released into solution.

© 2014 The Author(s) This is an Open Access article distributed under the terms of the Creative Commons Attribution Licence (CC-BY) (http://creativecommons.org/licenses/by/3.0/) which permits unrestricted use, distribution and reproduction in any medium, provided the original work is properly cited.

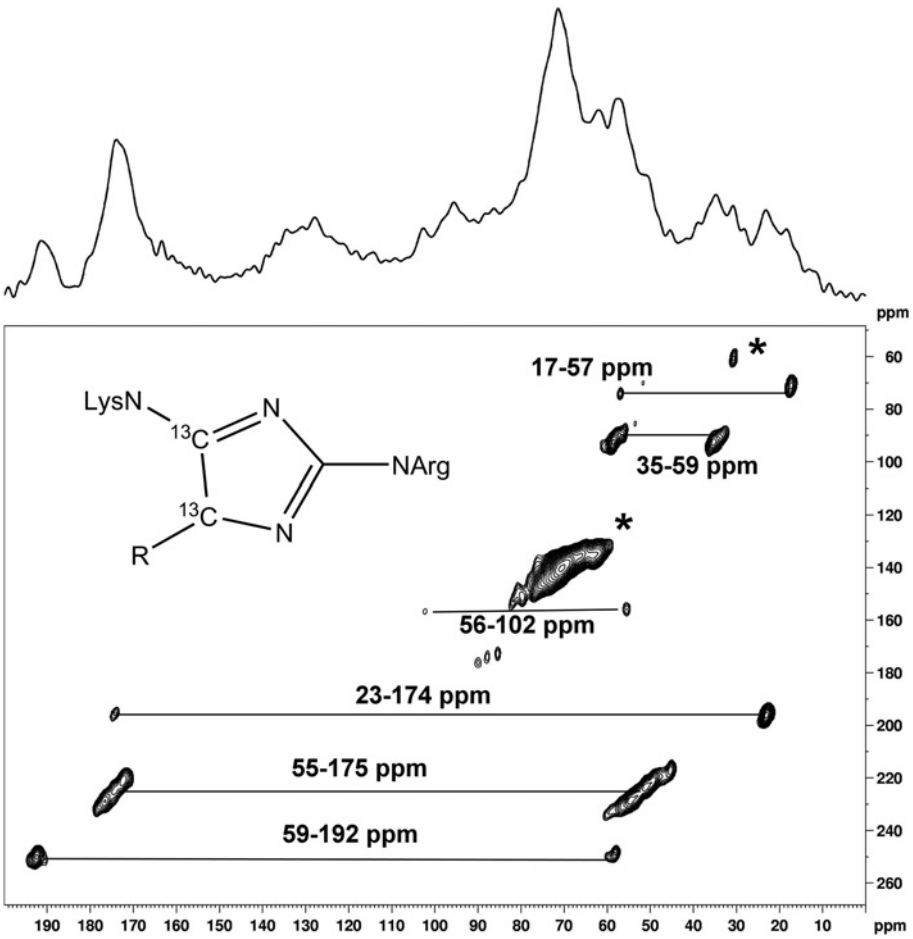

Figure 4 **2D ssNMR characterization of [U-^{13}C]ribose glycated collagen**
^{13}C ssNMR SQ–DQ (POST-C7) spectrum of [U-^{13}C]ribose glycated collagen, in which correlations are seen only between carbon atoms directly bonded to each other. The output of this experiment is presented as a contour plot in which the horizontal axis corresponds to the 1D SQ–DQ spectrum (plotted above the 2D spectrum), and the vertical axis to a 'double quantum' dimension. In effect the horizontal chemical shift coordinate of each cross peak corresponds to the shift of one or other of the directly bonded carbons, and the vertical coordinate to the sum of both shifts. Relevant frequency pairings are indicated. Note that the correlation labelled '55–175 ppm' corresponds to several correlations over a range of frequencies. Only species derived from the $^{13}C_5$-ribose molecule will give signals in this spectrum. The inset depicts the imidazole lysine-arginine crosslink motif, which leads to a POST-C7 correlation between the carboxyimidamide carbon at ~175 ppm and the adjacent amino carbon at ~55 ppm. The possible AGEs with such a motif are DOPDIC (R = $CH_2CH(OH)CH_2OH$), which is derived directly from ribose, GODIC (R = H), derived from glyoxal and MODIC (R = Me), derived from methylglyoxal. Some signals (asterisked) correspond to 'autocorrelations' between signals from directly bonded carbons with very similar or identical chemical shifts. See Table 2 for assignments.

The soluble AGEs produced from ribosylation of collagen bear limited resemblance to those produced by the PLL model. This shows that PLL does not completely mimic the Maillard reactions of collagen, and a more sophisticated model system is required to help determine the species present in the supernatant. In particular PLL does not replicate the considerable proportion of glycation-reactive arginyl residues in collagen (ca. 5 % versus about 3.5 % lysine in Type I collagen). It is also devoid of other amino acid functionalities, post-translational modifications and stable higher order structures (such as the collagen triple helices and fibril aggregates), any of which may exert unknown influences on glycation reactions, and increase glycation product diversity. It is interesting to note that very little of the acetic and formic acids that might have been expected as a result of the model systems are observed in the supernatant.

Collagen glycation by R5P

Under biomimetic reaction conditions, changes in collagen due to unlabelled R5P glycation were hard to detect by ssNMR beyond a general reduction in ^{13}C linewidths. Thus in order to observe glycation products more easily, the reaction was facilitated through slightly more basic (pH 9) conditions and sonicating the collagen to disperse it and ensure as many reactive (lysyl, arginyl) residues as possible were accessible for reaction.

© 2014 The Author(s) This is an Open Access article distributed under the terms of the Creative Commons Attribution Licence (CC-BY) (http://creativecommons.org/licenses/by/3.0/) which permits unrestricted use, distribution and reproduction in any medium, provided the original work is properly cited.

Table 2 A summary of the ^{13}C POST-C_7 correlations observed in collagen glycated by [U-^{13}C]ribose over 69 days, with assignments

POST-C_7 correlations	Assignment	
Signal 1/ppm	Signal 2/ppm	
17	57	MODIC and/or CEL
23	174	N^{ε}-acetyl lysine or acetic acid
31	31	?
35	59	DOPDIC and/or pentosinane
45–60	170–180	DOPDIC, MODIC, GODIC, pentosinane, CML, CEL
56	102	ribuloselysine
59	192	'norpronyl-lysine'
65–75	65–75	Any vicinal diol
88	88	?

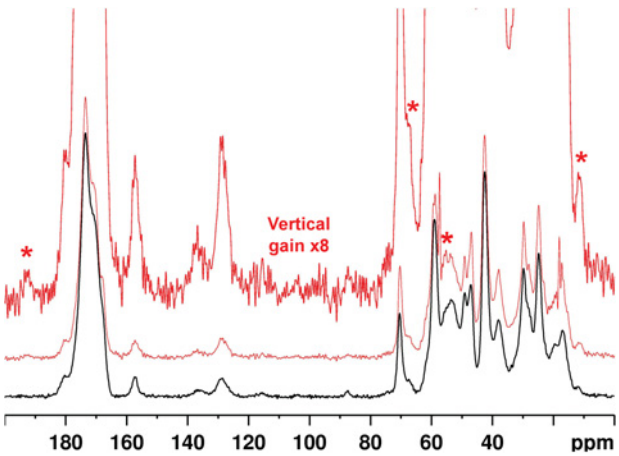

Figure 5 ^{13}C ssNMR characterization of collagen glycation by R5P
^{13}C ssNMR spectrum of collagen after 14 days incubation (black, bottom trace), and collagen glycated by R5P for the same period after sonication and at pH9 (red, upper traces). Asterisked areas indicate where new signal appears from AGEs, identified in all cases by signal-to-noise ratios of greater than 2. The sharp signals at 18 and 58 ppm are due to ethanol present as an impurity in the R5P commercial starting material; that they persist after several washes implies the ethanol is closely bound into the collagen matrix.

The results of collagen glycation by R5P are shown in Figure 5. The slight sharpening of collagen signals is attributed to an increase in molecular hydration and molecular mobility after sonication and glycation. Areas where there appears to be new AGE signals are asterisked. The 12, 68 and 192 ppm signals are also present in PLL after R5P glycation. The prominence of 192 ppm suggests norpronyl-lysine is again present as an important AGE. The 12 ppm signal could be from norpronyl-lysine, MODIC, CEL or a combination thereof. The 68 ppm signal could be from any of the various AGEs containing an alcohol group. The 56 ppm signal is currently unassigned, and it is unclear whether this is a genuine AGE signal or a collagen signal which becomes apparent from the reduction in linewidths for the sonicated, glycated sample.

DISCUSSION

NMR in both the liquid and solid phases is well known as a technique giving detailed chemical information on the composition of biological fluids and tissues in a near-native state. Characterization generally does not require separation of components, prior assumptions about possible composition, or that molecules of interest fortuitously possess distinctive spectroscopic 'marker' properties such as fluorescence. These factors have facilitated identification of a new glycation product arising from ribose and R5P glycation for which we propose the common name norpronyl lysine, and some previously unknown and unexpected aspects of biological glycation processes and products, such as amine catalysed sugar epimerizations under mild, approximately biological conditions.

Ribose [35], and especially R5P and ADPR [36–38], are vigorous glycating chemicals. Ribose and R5P are ubiquitous and key intermediates in several biochemical pathways including nucleotide biosynthesis and degradation and the pentose phosphate pathway, and can act as important carbon and energy sources. R5P attains significant levels greater than approximately millimolar in some tissues [39], certainly high enough to raise the possibility of its acting as a reactive glycating agent. Type 2 diabetes is characterized by activation of multiple inflammatory processes, mediators and pathways [40,41]; vascular damage leading to atherosclerosis is a typical pathological consequence [42] partly mediated in fact by specific RAGE (receptor of AGE) which initiate further cascades of inflammation [43].

ADPR and PAR (poly-ADP-ribose) are long recognized major components in crucial cell signalling, control and repair pathways [44], and there are intensive efforts to discover pharmacological modulators [45]. Potential benefits include down-regulation of multiple parallel pathways of inflammation and tissue injury in, for instance, diabetic complications. Important components of these pathways include enzymes such as PARG (PAR glycohydrolase) [46] and ADP-ribosyl protein lyase, which rapidly [44] generate free ADPR from PAR. This hydrolysis exposes the reactive ribosyl 1″-anomeric carbons, which are protected by glycosidic conjugation in PAR. The reactive species, normally intracellular, will flood out of necrotizing cells and be able to react with extracellular matrix, which they will do much faster than the comparatively stable glucose.

In addition to the real possibility of these pentose sugars and their derivatives acting as significant glycating agents in their own right, the reactions they undergo with proteins reproduce mechanistically many if not all of the glycating actions of generally more abundant but much more sluggish reactants such as glucose and other hexoses and hexose phosphates. This not only makes the pentoses attractive reagents for understanding the nature and effects of the more abundant sugars, it raises the possibility of performing *in vitro* whole tissue or even *in vivo* experiments with

© 2014 The Author(s) This is an Open Access article distributed under the terms of the Creative Commons Attribution Licence (CC-BY) (http://creativecommons.org/licenses/by/3.0/) which permits unrestricted use, distribution and reproduction in any medium, provided the original work is properly cited.

labelled reactive glycating agents with subsequent *ex vivo* NMR and other, e.g. MS, analyses greatly facilitated by the resultant increase in sensitivity and discriminating power.

AUTHOR CONTRIBUTION

Peter Bullock performed experiments, analysis and made a contribution to preparing the paper. David Reid conceived the study with Melinda Duer, and contributed to experiment design, implementation and interpretation, and preparing the paper. W. Ying Chow set up and optimized solid-state NMR methodology. Wendy Lau performed and analysed some experiments. Melinda Duer contributed to study conception and preparation of the paper.

ACKNOWLEDGEMENTS

We thank Dr Peter Grice, Duncan Howe and Andrew Mason for acquisition of solution state NMR data.

FUNDING

This work was supported by the U.K. Medical Research Council (MRC) [grant number MR/J007692/1 (to D.G.R.)], and Engineering and Physical Sciences Research Council (EPSRC) [general DTA fund (to W.Y.C.)].

REFERENCES

1 Huebschmann, A. G., Regensteiner, J. G., Vlassara, H. and Reusch, J. E. B. (2006) Diabetes and advanced glycoxidation end products. Diab. Care **29**, 1420–1432
2 Monnier, V. M., Sell, D. R., Nagaraj, R. H., Miyata, S., Grandhee, S., Odetti, P. and Ibrahim, S. A. (1992) Maillard reaction-mediated molecular damage to extracellular-matrix and other tissue proteins in diabetes, aging, and uremia. Diabetes **41**, 36–41
3 Avery, N. C. and Bailey, A. J. (2005) Enzymic and non-enzymic cross-linking mechanisms in relation to turnover of collagen: relevance to aging and exercise. Scand. J. Med. Sci. Sports **15**, 231–240
4 Sandwick, R., Johanson, M. and Breuer, E. (2005) Maillard reactions of ribose 5–phosphate and amino acids. Ann. N. Y. Acad. Sci. **1043**, 85–96
5 Munanairi, A., O'Banion, S. K., Gamble, R., Breuer, E., Harris, A. W. and Sandwick, R. K. (2007) The multiple Maillard reactions of ribose and deoxyribose sugars and sugar phosphates. Carbohydr. Res. **342**, 2575–2592
6 Wrobel, K., Wrobel, K., Garay-Sevilla, M. E., Nava, L. E. and Malacara, J. M. (1997) Novel analytical approach to monitoring advanced glycosylation end products in human serum with on-line spectrophotometric and spectrofluorometric detection in a flow system. Clin. Chem. **43**, 1563–1569
7 Kume, S., Takeya, M., Mori, T., Araki, N., Suzuki, H., Horiuchi, S., Kodama, T., Miyauchi, Y. and Takahashi, K. (1995) Immunohistochemical and ultrastructural detection of advanced glycation end-products in atherosclerotic lesions of human aorta with a novel specific monoclonal-antibody. Am. J. Pathol. **147**, 654–667
8 Vallejo-Cordoba, B. and Gonzalez-Cordova, A. F. (2007) CE: A useful analytical tool for the characterization of Maillard reaction products in foods. Electrophoresis **28**, 4063–4071
9 Dunn, J. A., Patrick, J. S., Thorpe, S. R. and Baynes, J. W. (1989) Oxidation of glycated proteins–age-dependent accumulation of N-epsilon-(carboxymethyl)lysine in lens proteins. Biochemistry **28**, 9464–9468
10 Sell, D. R., Biemel, K. M., Reihl, O., Lederer, M. O., Strauch, C. M. and Monnier, V. M. (2005) Glucosepane is a major protein cross-link of the senescent human extracellular matrix–relationship with diabetes. J. Biol. Chem. **280**, 12310–12315
11 Biemel, K. M., Reihl, O., Conrad, J. and Lederer, M. O. (2001) Formation pathways for lysine-arginine cross-links derived from hexoses and pentoses by Maillard processes–unravelling the structure of a pentosidine precursor. J. Biol. Chem. **276**, 23405–23412
12 Biemel, K. M., Conrad, J. and Lederer, M. O. (2002) Unexpected carbonyl mobility in aminoketoses: the key to major Maillard crosslinks. Angew. Chem. Int. Ed. Engl. **41**, 801–803
13 Wells-Knecht, K. J., Zyzak, D. V., Litchfield, J. E., Thorpe, S. R. and Baynes, J. W. (1995) Mechanism of autoxidative glycosylation–identification of glyoxal and arabinose as intermediates in the autoxidative modification of proteins by glucose. Biochemistry **34**, 3702–3709
14 Wells-Knecht, M. C., Thorpe, S. R. and Baynes, J. W. (1995) Pathways of formation of glycoxidation products during glycation of collagen. Biochemistry **34**, 15134–15141
15 Ferreira, A. E. N., Freire, A. M. J. P. and Voit, E. O. (2003) A quantitative model of the generation of N-epsilon-(carboxymethyl)lysine in the Maillard reaction between collagen and glucose. Biochem. J. **376**, 109–121
16 Chuyen, N. V., Kurata, T. and Fujimaki, M. (1973) Formation of N-carboxymethyl amino-acid from reaction of alpha-amino-acid with glyoxal. Agric. Biol. Chem. **37**, 2209–2210
17 Smuda, M., Voigt, M. and Glomb, M. A. (2010) Degradation of 1–deoxy-D-erythro-hexo-2,3-diulose in the presence of lysine leads to formation of carboxylic acid amides. J. Agric. Food Chem. **58**, 6458–6464
18 Henning, C., Smuda, M., Girndt, M., Ulrich, C. and Glomb, M. A. (2011) Molecular Basis of Maillard amide-advanced glycation end product (AGE) formation *in Vivo*. J. Biol. Chem. **286**, 44350–44356
19 Monnier, V. M., Mustata, G. T., Biemel, K. L., Reihl, O., Lederer, M. O., Dai, Z. Y. and Sell, D. R. (2005) Cross-linking of the extracellular matrix by the Maillard reaction in aging and diabetes–An update on 'a puzzle nearing resolution'. Ann. N. Y. Acad. Sci. **1043**, 533–544
20 Rizzi, G. P. (2004) Role of phosphate and carboxylate ions in Maillard browning. J. Agric. Food Chem. **52**, 953–957
21 Delatour, T., Fenaille, F., Parisod, V., Vera, F. A. and Buetler, T. (2006) Synthesis, tandem MS- and NMR-based characterization, and quantification of the carbon 13–labeled advanced glycation endproduct, 6–N-carboxymethyllysine. Amino Acids **30**, 25–34
22 Maekawa, Y., Sugiura, M., Takeuchi, A., Tomoo, K., Ishida, T. and Kamigauchi, M. (2010) Study of lysozyme glycation reaction by mass spectrometry and NMR spectroscopy. Helvet. Chim. Acta **93**, 991–998
23 Howard, M. J. and Smales, C. M. (2005) NMR analysis of synthetic human serum albumin alpha-helix 28 identifies structural distortion upon Amadori modification. J. Biol. Chem. **280**, 22582–22589
24 Hohwy, M., Jakobsen, H. J., Eden, M., Levitt, M. H. and Nielsen, N. C. (1998) Broadband dipolar recoupling in the nuclear magnetic resonance of rotating solids: a compensated C7 pulse sequence. J. Chem. Phys. **108**, 2686–2694
25 King-Morris, M. J. and Serianni, A. S. (1987) C-13 NMR-studies of [1-C-13]aldoses-empirical rules correlating pyranose ring configuration and conformation with C-13 chemical-shifts and C-13-C-13 spin couplings. J. Am. Chem. Soc. **109**, 3501–3508
26 Gleason, W. B. and Barker, R. (1971) Evidence for a hydride shift in alkaline rearrangements of D-ribose. Can. J. Chem. **49**, 1433–1440

© 2014 The Author(s) This is an Open Access article distributed under the terms of the Creative Commons Attribution Licence (CC-BY) (http://creativecommons.org/licenses/by/3.0/) which permits unrestricted use, distribution and reproduction in any medium, provided the original work is properly cited.

27 Hellwig, M. and Henle, T. (2010) Formyline, a new glycation compound from the reaction of lysine and 3-deoxypentosone. Eur. Food Res. Technol. **230**, 903–914
28 Cistola, D. P., Small, D. M. and Hamilton, J. A. (1982) Ionization behavior of aqueous short-chain carboxylic-acids–a C-13 NMR-study. J. Lipid Res. **23**, 795–799
29 Hagen, R. and Roberts, J. D. (1969) Nuclear magnetic resonance spectroscopy. ^{13}C spectra of aliphatic carboxylic acids and carboxylate anions. J. Am. Chem. Soc. **91**, 4504–4506
30 Zou, J., Guo, Z. J., Parkinson, J. A., Chen, Y. and Sadler, P. J. (1999) Gold(III)-induced oxidation of glycine. Chem. Commun. 1359–1360
31 Hauck, T., Hubner, Y., Bruhlmann, F. and Schwab, W. (2003) Alternative pathway for the formation of 4,5–dihydroxy-2,3-pentanedione, the proposed precursor of 4-hydroxy-5-methyl-3(2H)-furanone as well as autoinducer-2, and its detection as natural constituent of tomato fruit. Biochim. Biophys. Acta–Gen. Subj. **1623**, 109–119
32 Panneerselvam, J., Aranganathan, S. and Nalini, N. (2009) Inhibitory effect of bread crust antioxidant pronyl-lysine on two different categories of colonic premalignant lesions induced by 1,2-dimethylhydrazine. Eur. J. Cancer Prev. **18**, 291–302
33 Brinkmann, E., Wells-Knecht, K. J., Thorpe, S. R. and Baynes, J. W. (1995) Characterization of an imidazolium compound formed by reaction of methylglyoxal and N-alpha-hippuryllysine. J. Chem. Soc., Perkin. Trans. **1**, 2817–2818
34 Wells-Knecht, K. J., Brinkmann, E. and Baynes, J. W. (1995) Characterization of an imidazolium salt formed from glyoxal and N-alpha-hippuryllysine–a model for Maillard reaction cross-links in proteins. J. Org. Chem. **60**, 6246–6247
35 Yan, H. and Harding, J. J. (1997) Glycation-induced inactivation and loss of antigenicity of catalase and superoxide dismutase. Biochem. J. **328**, 599–605
36 Cervantes-Laurean, D., Jacobson, E. L. and Jacobson, M. K. (1996) Glycation and glycoxidation of histones by ADP-ribose. J. Biol. Chem. **271**, 10461–10469
37 Schreiber, V., Dantzer, F., Ame, J. C. and de Murcia, G. (2006) Poly(ADP-ribose): novel functions for an old molecule. Nat. Rev. Mol. Cell Biol. **7**, 517–528
38 Jacobson, E. L., Cervantes-Laurean, D. and Jacobson, M. K. (1994) Glycation of proteins by ADP-ribose. Mol. Cell. Biochem. **138**, 207–212
39 Camici, M., Tozzi, M. G. and Ipata, P. L. (2006) Methods for the determination of intracellular levels of ribose phosphates. J. Biochem. Biophys. Methods **68**, 145–154
40 Donath, M. Y. and Shoelson, S. E. (2011) Type 2 diabetes as an inflammatory disease. Nat. Rev. Immunol. **11**, 98–107
41 Wellen, K. E. and Hotamisligil, G. S. (2005) Inflammation, stress, and diabetes. J. Clin. Invest. **115**, 1111–1119
42 Goldin, A., Beckman, J. A., Schmidt, A. M. and Creager, M. A. (2006) Advanced glycation end products–sparking the development of diabetic vascular injury. Circulation **114**, 597–605
43 Park, L., Raman, K. G., Lee, K. J., Lu, Y., Ferran, L. J., Chow, W. S., Stern, D. and Schmidt, A. M. (1998) Suppression of accelerated diabetic atherosclerosis by the soluble receptor for advanced glycation endproducts. Nat. Med. **4**, 1025–1031
44 Juarez-Salinas, H., Sims, J. L. and Jacobson, M. K. (1979) Poly(ADP-Ribose) levels in carcinogen-treated cells. Nature **282**, 740–741
45 Jagtap, P. and Szabo, C. (2005) Poly(ADP-ribose) polymerase and the therapeutic effects of its inhibitors. Nat. Rev. Drug Discov. **4**, 421–440
46 Davidovic, L., Vodenicharov, M., Affar, E. B. and Poirier, G. G. (2001) Importance of poly(ADP-ribose) glycohydrolase in the control of poly(ADP-ribose) metabolism. Exp. Cell Res. **268**, 7–13

Received 11 December 2013/15 January 2014; accepted 29 January 2014

Published as Immediate Publication 12 February 2014, doi 10.1042/BSR20130135

© 2014 The Author(s) This is an Open Access article distributed under the terms of the Creative Commons Attribution Licence (CC-BY) (http://creativecommons.org/licenses/by/3.0/) which permits unrestricted use, distribution and reproduction in any medium, provided the original work is properly cited.

Biosci. Rep. (2014) / **34** / art:e00096 / doi 10.1042/BSR20130135

OPEN ACCESS

Original Paper

SUPPLEMENTARY DATA

A new glycation product 'norpronyl-lysine,' and direct characterization of cross linking and other glycation adducts: NMR of model compounds and collagen

Peter T. B. BULLOCK*, David G. REID*, W. YING CHOW*, Wendy P. W. LAU* and Melinda J. DUER*[1]

*Department of Chemistry, University of Cambridge, Lensfield Road, Cambridge CB2 1EW, U.K.

AGE formation

An ever growing number of AGEs have been identified and characterised in the last 20 years [1–6]. The many possible reaction pathways the initial Amadori product can explore is reflected in the structural variety of AGEs discovered so far (Figure S1).

Put broadly, the possible reaction routes fall into three groups, anticipated as early as 1953 [7].

The first category, that of products formed via formation of a reactive α-dicarbonyl species, is exemplified by pentosidine, a reaction product of pentose sugars [8]. This sort of α-dicarbonyl mechanism also leads to the formation of 4-hydroxyl-5-methyl-3(2H)-furanone (norfuraneol) from ribose as shown in Scheme S2 [9].

The second category involves fragmentation of the sugar carbon chain by retro-aldol reaction, hydrolytic cleavage or oxidative cleavage. The reactive sugar degradation products glyoxal and methylglyoxal in particular play a role in the formation of many AGEs. The two pathways to formation of CML [10,11] are a good example (Scheme S3), with oxidative cleavage of the Amadori product [3] competing with reaction of lysine with glyoxal [12].

Recently a third category of AGE has been discovered *in vitro* and *in vivo*: that of carboxylic amides, derived from β-dicarbonyl cleavage (Scheme S4) [13]. Of these N^{ε}-acetyl lysine and N^{ε}-formyl lysine are present in human plasma at comparable levels to CML [14].

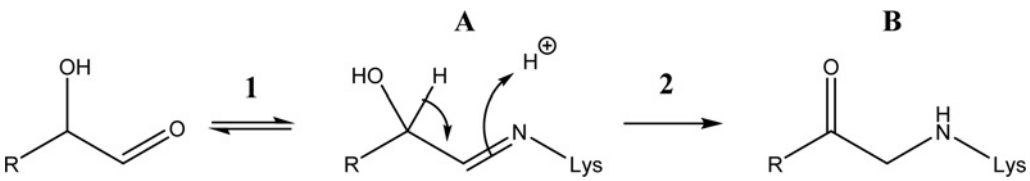

Scheme S1 **The Maillard reaction occurs in three stages**
Firstly, the sugar carbonyl group condenses with a terminal amine group (usually from a lysine residue) giving a Schiff base, (**A**) This subsequently undergoes an Amadori rearrangement yielding the more stable ketosamine (**B**). The ketosamine can then undergo a variety of transformations giving a plethora of AGEs.

[1] To whom correspondence should be addressed (email mjd13@cam.ac.uk).

© 2014 The Author(s) This is an Open Access article distributed under the terms of the Creative Commons Attribution Licence (CC-BY) (http://creativecommons.org/licenses/by/3.0/) which permits unrestricted use, distribution and reproduction in any medium, provided the original work is properly cited.

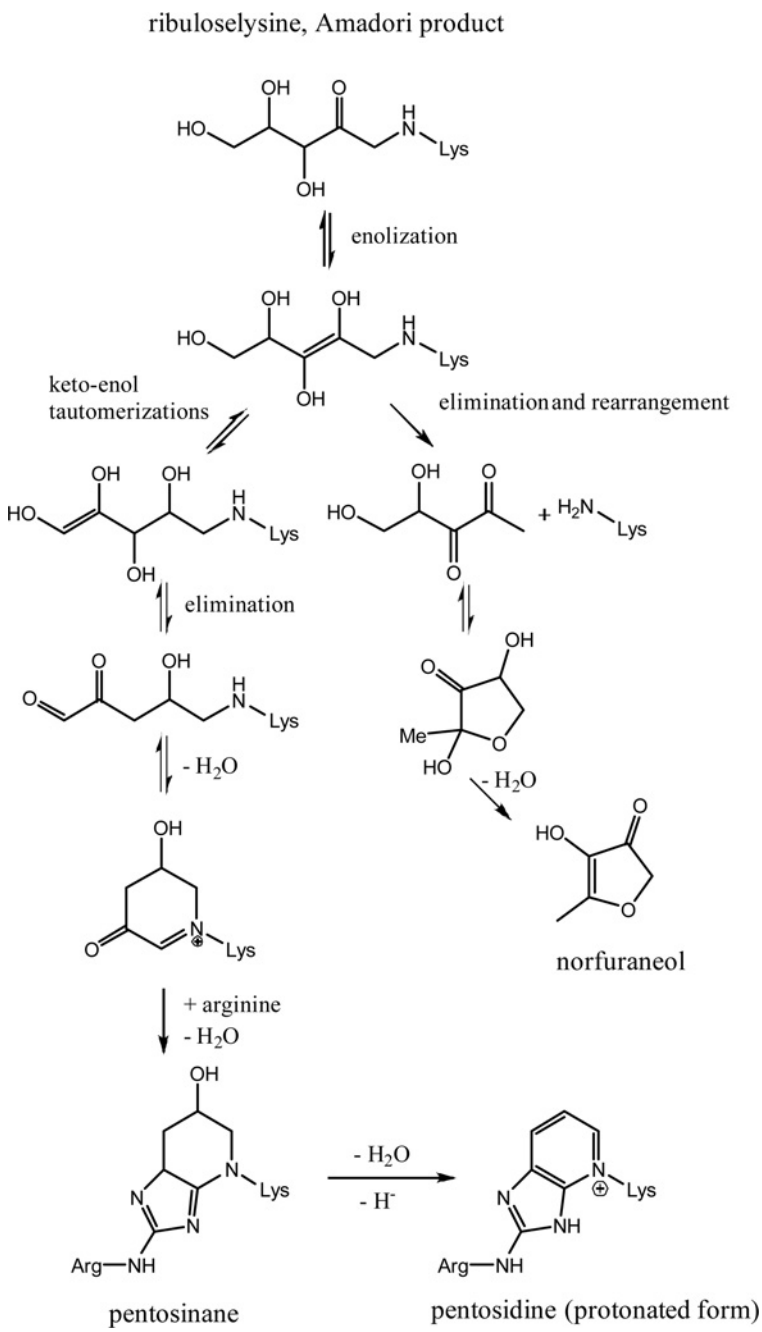

Scheme S2 **Mechanisms of formation of pentosinane, pentosidine and norfuraneol from ribuloselysine, the Amadori product of ribose and lysine**

© 2014 The Author(s) This is an Open Access article distributed under the terms of the Creative Commons Attribution Licence (CC-BY) (http://creativecommons.org/licenses/by/3.0/) which permits unrestricted use, distribution and reproduction in any medium, provided the original work is properly cited.

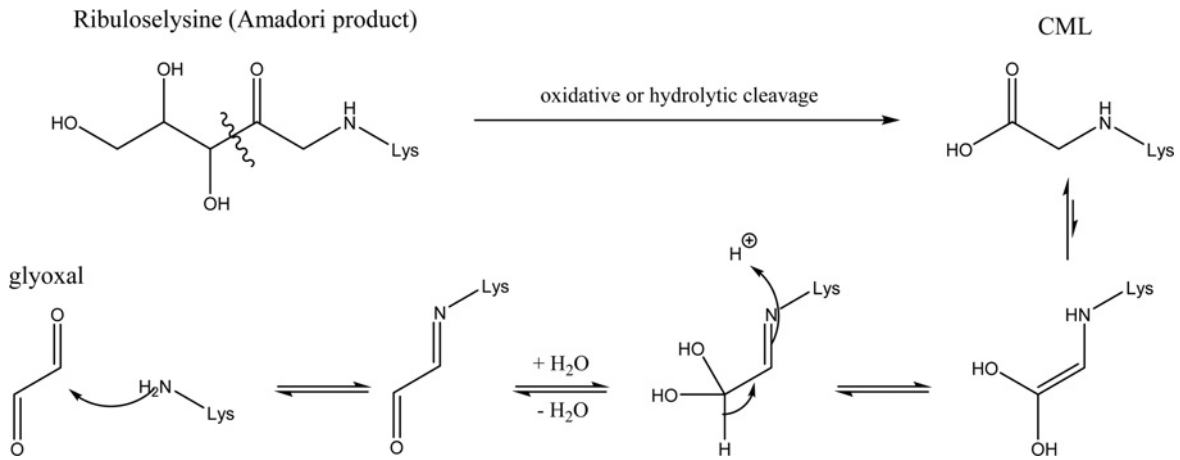

Scheme S3 **Mechanisms of formation of CML**
The pathway which dominates has been shown to depend on phosphate concentration and sugar concentration, with the glyoxal route dominant except at low phosphate and high sugar [10,11].

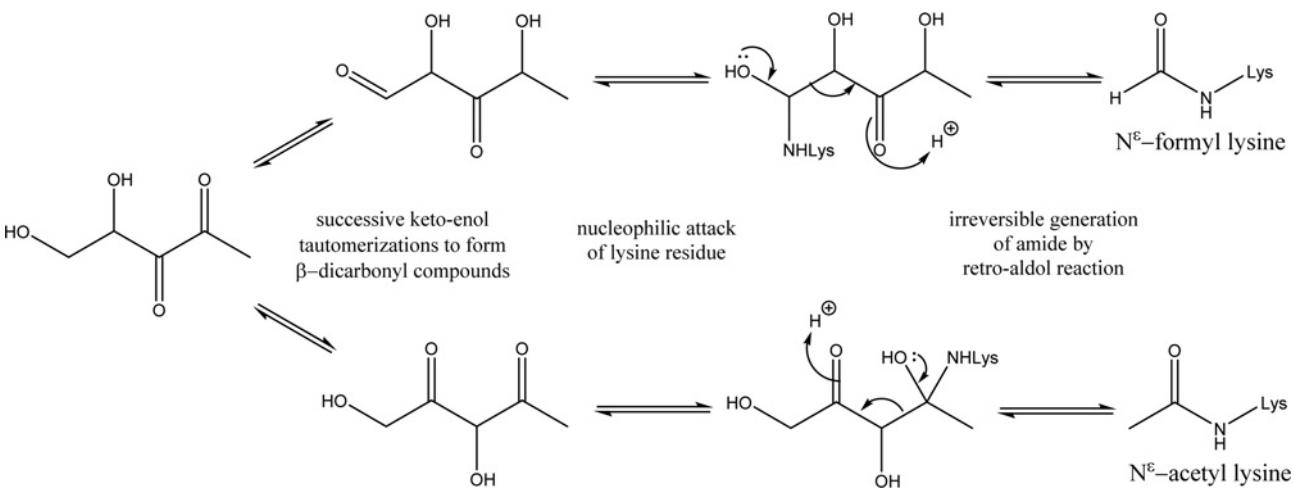

Scheme S4 **Mechanism of formation of N^{ε}-acetyl lysine and N^{ε}-formyl lysine from ribose**
The shown starting material is a degradation product of ribuloselysine (Scheme S2). N^{ε}-lactoyl lysine and N^{ε}-glycolyl lysine can also be formed if the lysine residue attacks the other carbonyl group in the β-dicarbonyl intermediate.

© 2014 The Author(s) This is an Open Access article distributed under the terms of the Creative Commons Attribution Licence (CC-BY) (http://creativecommons.org/licenses/by/3.0/) which permits unrestricted use, distribution and reproduction in any medium, provided the original work is properly cited.

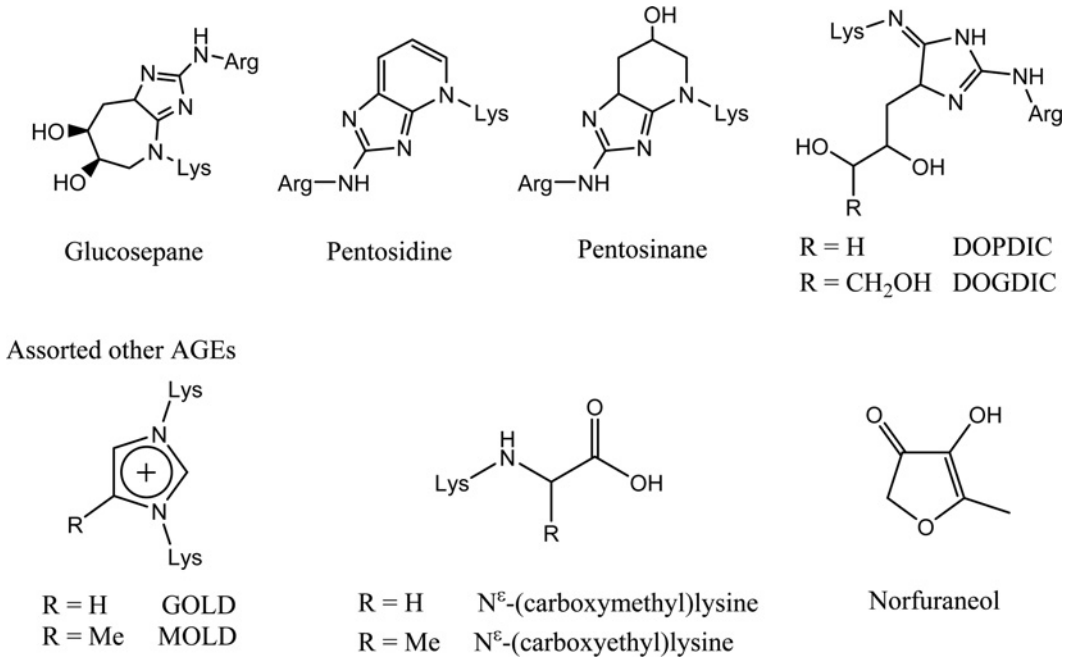

Figure S1 **Some important AGEs**

Glucosepane is considered the most important known crosslink [10], being derived from glucose. Pentosidine and its precursor pentosinane are formed in the same manner as glucosepane from pentose sugars (which are formed by the autoxidation of glucose). **DOGDIC** (N6-{2-{[(4S)-4-ammonio-5-oxido-5-oxopentyl]amino}-5-[(2S,3R)-2,3,4-trihydroxybutyl]-3,5-dihydro-4H-imidazol-4-ylidene}-L-lysinate) and **DOPDIC** are hydrolysed forms of glucosepane and pentosinane, respectively. **GOLD** and N^{ε}-**CML** are the products formed by reaction of lysine with glyoxal (a product from the oxidation of sugars). MOLD (methylglyoxal lysine dimer) and N^{ε}-**CEL** are the analogous products formed from methylglyoxal (a product from the fragmentation of sugars). Norfuraneol is formed from the amine-catalysed rearrangement and dehydration of pentose sugars.

© 2014 The Author(s) This is an Open Access article distributed under the terms of the Creative Commons Attribution Licence (CC-BY) (http://creativecommons.org/licenses/by/3.0/) which permits unrestricted use, distribution and reproduction in any medium, provided the original work is properly cited.

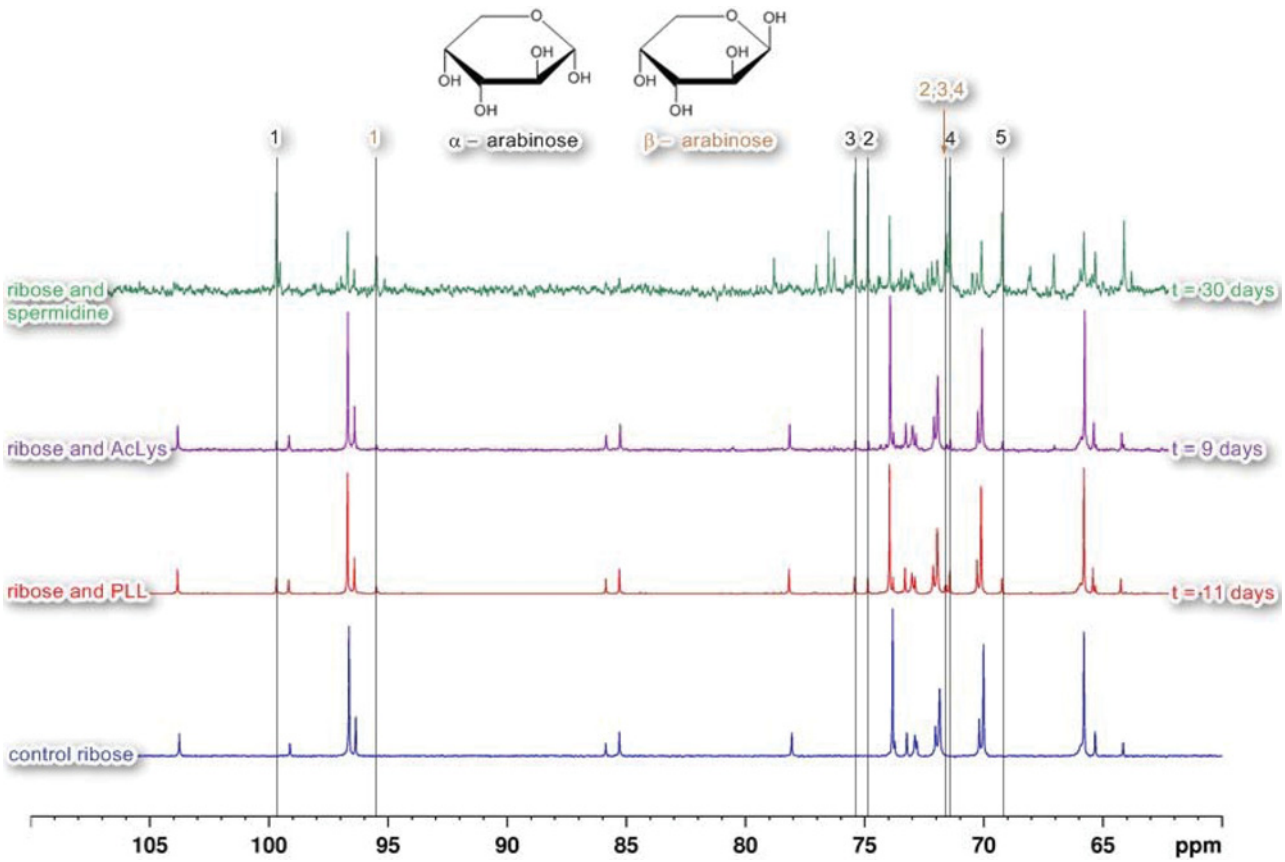

Figure S2 **^{13}C solution-state NMR spectra of incubations of ribose with (a) spermidine after 30 days (green), (b) AcLys after 9 days (purple), (c) PLL after 11 days (red) and (d) no amine present (blue)**
In each case the peaks at δ69.2, 71.5 (multiple), 74.8, 75.4, 95.5 and 99.7 ppm which are not present in a control incubation of ribose in the absence of amine are diagnostic of formation of arabinose, the C2-epimer of ribose,with the assignments given.

© 2014 The Author(s) This is an Open Access article distributed under the terms of the Creative Commons Attribution Licence (CC-BY) (http://creativecommons.org/licenses/by/3.0/) which permits unrestricted use, distribution and reproduction in any medium, provided the original work is properly cited.

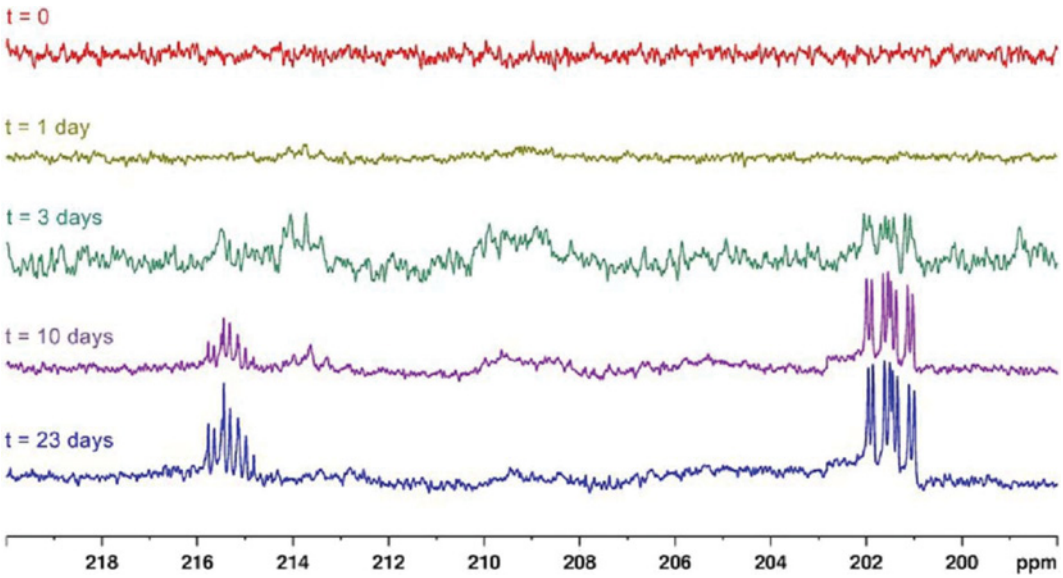

Figure S3 **^{13}C solution-state NMR spectra of the reaction between [U-^{13}C]ribose and PLL with data taken over a period of 23 days**

The broad signal at 209 ppm, assigned to the carbonyl carbon of ribuloselysine, the Amadori product, reaches a maximum after 3 days before slowly decaying, although it is still present after 23 days suggesting the glycation process had not yet gone to completion. The broadness of the signal is presumably attributable to the polymeric nature of PLL: each ribuloselysine entity is in a slightly different chemical environment. The multiplet (doublet of doublets of doublet) at 202 ppm couples to 136 ppm and is from norfuraneol. The multiplet around 215 ppm is from relatively stable ketone intermediates; a corresponding feature is also present in reactions of R5P.

© 2014 The Author(s) This is an Open Access article distributed under the terms of the Creative Commons Attribution Licence (CC-BY) (http://creativecommons.org/licenses/by/3.0/) which permits unrestricted use, distribution and reproduction in any medium, provided the original work is properly cited.

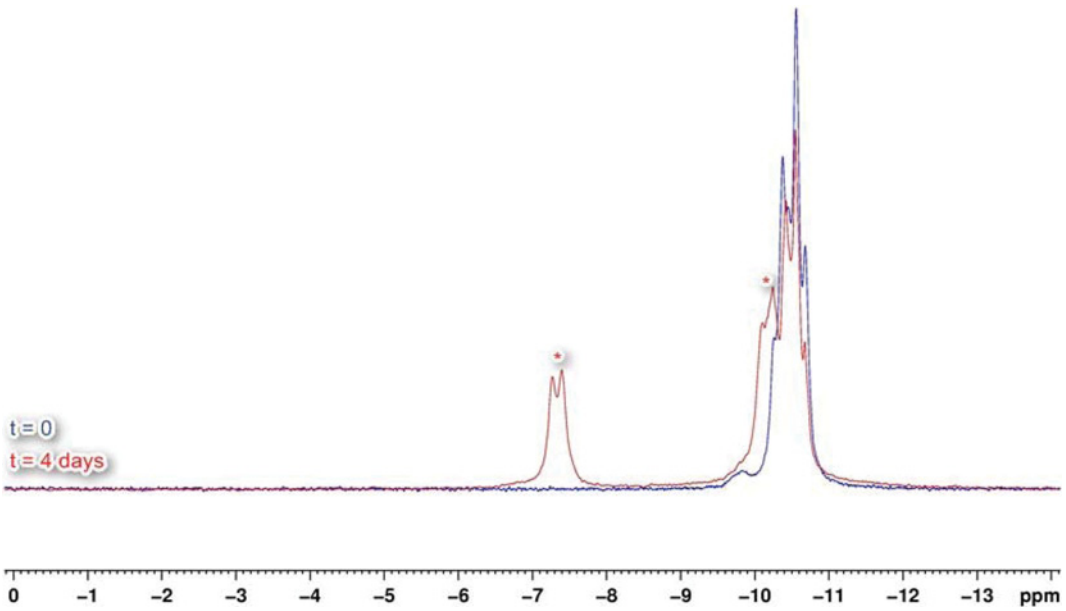

Figure S4 **^{31}P solution-state NMR of ADPR before (blue) and after (red) reaction with PLL**

The ADPR signal loses intensity and is replaced with two doublets (asterisked) at −7.3 and −10.2 ppm (J = 20 Hz) which correspond to the β- and α-phosphate groups of free ADP, released from ADPR, respectively.

© 2014 The Author(s) This is an Open Access article distributed under the terms of the Creative Commons Attribution Licence (CC-BY) (http://creativecommons.org/licenses/by/3.0/) which permits unrestricted use, distribution and reproduction in any medium, provided the original work is properly cited.

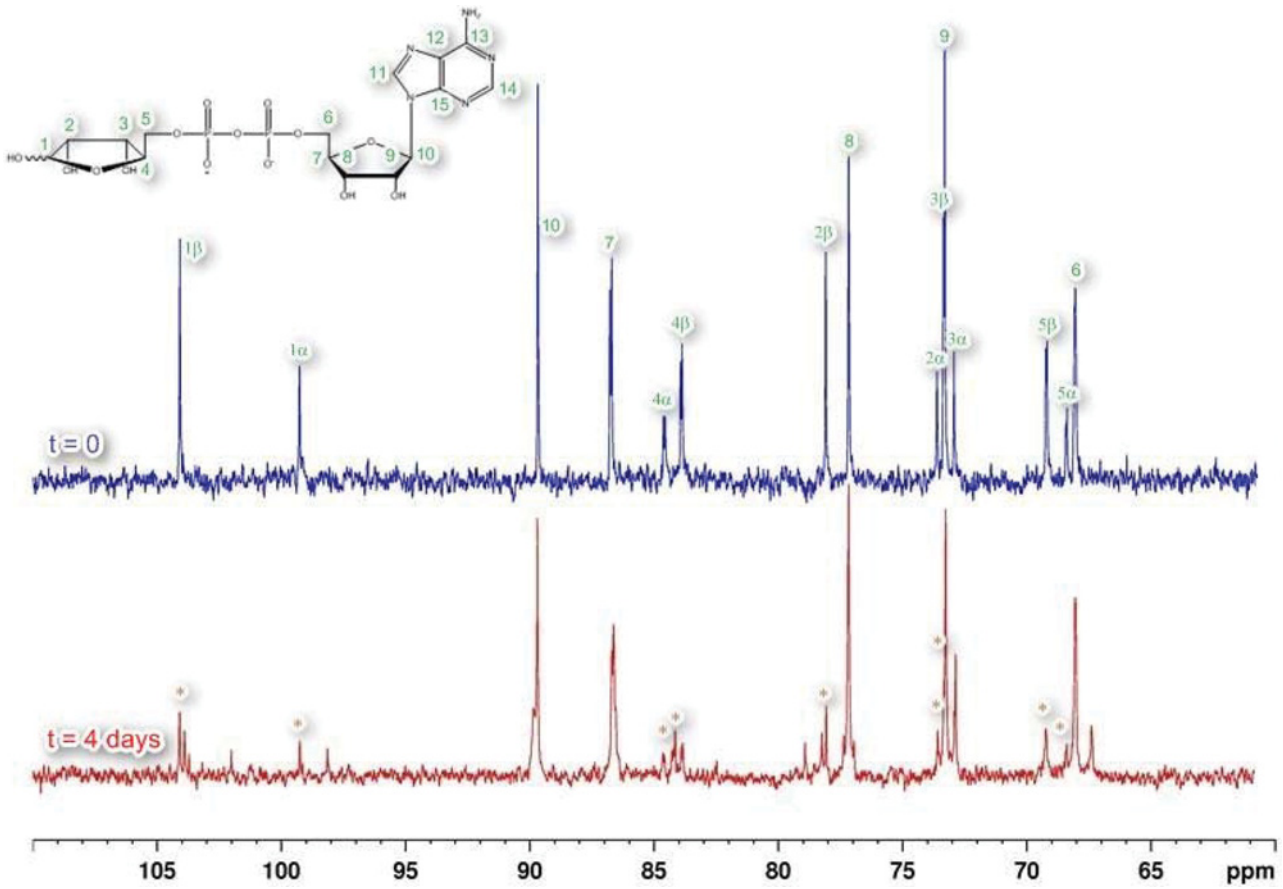

Figure S5 **^{13}C solution-state NMR of ADPR before (blue) and after (red) reaction with PLL**

ADPR assignment is given. The chemical shifts of C_1–C_5 of the ribosyl phosphate moiety are dependent on the configuration of the anomeric carbon, C_1, and accordingly signals from the α-anomer (hydroxyl group 'down') and the β-anomer (hydroxyl group 'up') are differentiated. After the generation of a precipitate (see text for details), the signals from the free ribose, asterisked, are significantly reduced, whereas the signals from ADP are unchanged in intensity. Taken with Figure S4, these results confirm that the ADP is released during the reaction that leads to crosslinking and precipitation. The same signal depletion over time was observed for glycation of PLL by R5P.

© 2014 The Author(s) This is an Open Access article distributed under the terms of the Creative Commons Attribution Licence (CC-BY) (http://creativecommons.org/licenses/by/3.0/) which permits unrestricted use, distribution and reproduction in any medium, provided the original work is properly cited.

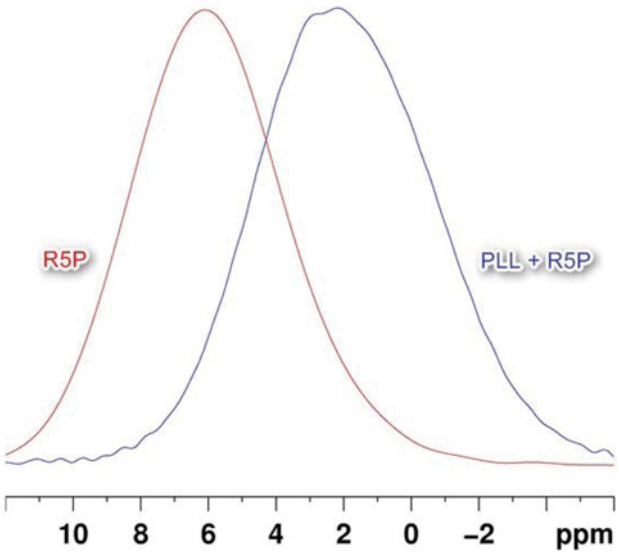

Figure S6 ^{31}P ssNMR of R5P before (red) and after (blue) reaction with PLL

The ^{31}P chemical shift changes from the phosphomonoester shift of 6.1–2.3 ppm of free phosphate ion. This further demonstrates that phosphate acts as a leaving group in the Maillard reactions of R5P.

© 2014 The Author(s) This is an Open Access article distributed under the terms of the Creative Commons Attribution Licence (CC-BY) (http://creativecommons.org/licenses/by/3.0/) which permits unrestricted use, distribution and reproduction in any medium, provided the original work is properly cited.

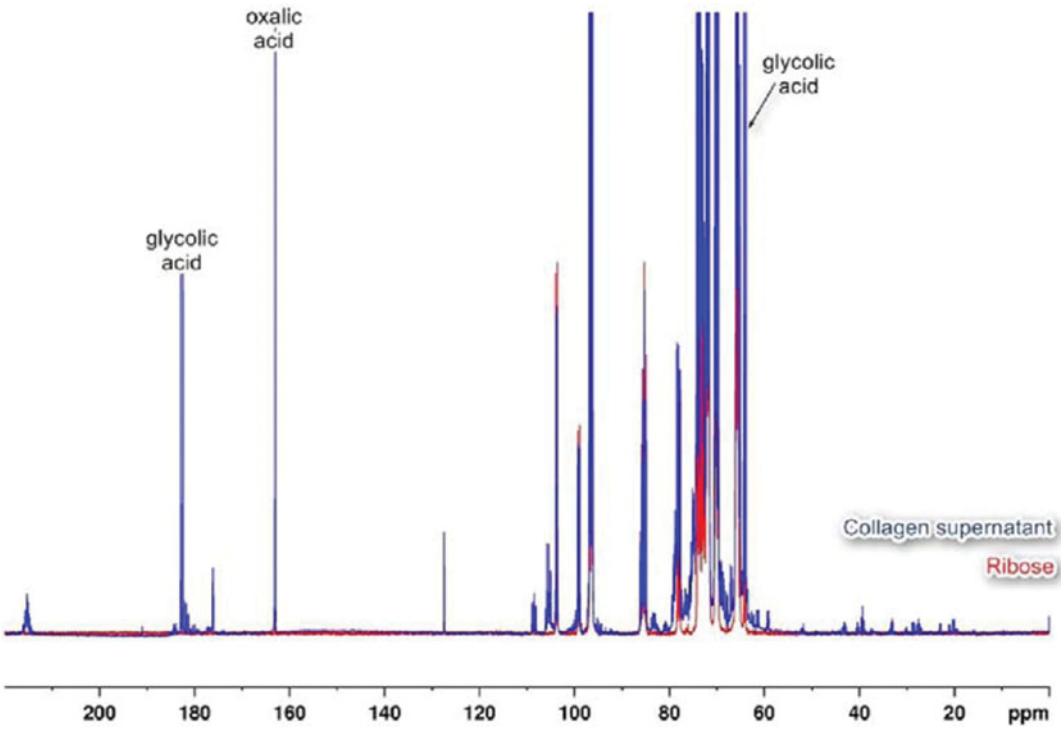

Figure S7 **^{13}C solution-state NMR spectrum of the supernatant phosphate buffer from [U-^{13}C]ribose glycated collagen (blue) and that of unreacted [U-^{13}C]ribose (red)**

The dominant species in the supernatant is unreacted ribose, but significant quantities of glycolic and oxalic acids were also observed (signals indicated, see Section 5.1.2), along with a multitude of weaker signals from minor AGEs which require further assignment.

© 2014 The Author(s) This is an Open Access article distributed under the terms of the Creative Commons Attribution Licence (CC-BY) (http://creativecommons.org/licenses/by/3.0/) which permits unrestricted use, distribution and reproduction in any medium, provided the original work is properly cited.

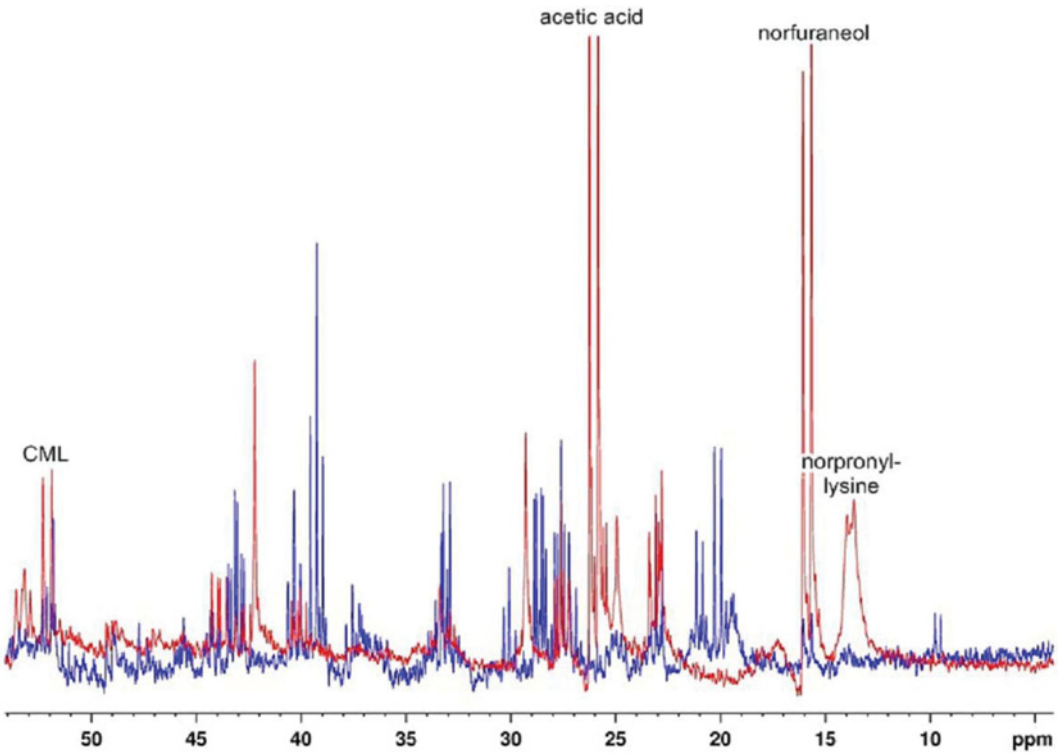

Figure S8 **Comparison of the ^{13}C NMR spectrum of the supernatant from [U-^{13}C]ribose glycated collagen (blue) and the model system: [U-^{13}C]ribose glycated PLL (red)**
Several weak signals are observed in both spectra, such the signal due to CML at 52 ppm. However, many of the supernatant AGE signals are not observed in the model system, showing that PLL is an incomplete model for collagen glycation. The lack of norpronyl-lysine in the supernatant is expected as it is attached to the solid collagen. The absence of norfuraneol and acetic acid is surprising: either they are not generated in observable quantities, or bind strongly to collagen, or had degraded by the time the spectrum was obtained.

Table S1 Shifts of C_1 and C_2 in carboxylic acids are highly pH and concentration dependent, with carboxylate ion C_1 typically resonating 4–5 ppm to higher frequency than the corresponding acid [15]
Values in the table are literature values for the acid form [16–18]. Formate resonated at 173.8 ppm, acetate at 184.1 and 26.1 ppm, glycolate at 182.6 and 62.1 ppm, oxalate at 163.0 ppm. Glyoxylate was not observed. These assignments were confirmed by peak multiplicity, *J* values, and ^{13}C–^{13}C COSY correlations, in isotopically enriched experiments.

	C_1 (ppm)	C_2 (ppm)
Formic acid	167	–
Acetic acid	178	22
Glycolic acid	177	60
Glyoxylic acid	174	90
Oxalic acid	161	161

© 2014 The Author(s) This is an Open Access article distributed under the terms of the Creative Commons Attribution Licence (CC-BY) (http://creativecommons.org/licenses/by/3.0/) which permits unrestricted use, distribution and reproduction in any medium, provided the original work is properly cited.

Table S2 A summary of the carboxylic acids generated in the Maillard reactions between model amines and sugars

A tick indicates that the species is appreciably present, a tick in parentheses that it is weak, a cross that there is no evidence of the species.

Reactants	Formic acid	Acetic acid	Glycolic acid	Glyoxylic acid	Oxalic acid
Ribose and PLL	√?	×	√	×	×
[U-^{13}C]-ribose and PLL	√	√	√	×	(√)
R5P and PLL	(√)	×	√	×	×
[U-^{13}C]-ribose and collagen	(√)	(√)	√	×	√
Ribose and AcLys	√	√	√	×	×
[U-^{13}C]-ribose and AcLys	√	√	√	×	(√)
R5P and AcLys	√	√	×	×	×
Ribose and spermidine	√	√	√	×	×

Table S3 Full ^{13}C solution-state NMR assignment of $^{13}C_5$-norfuraneol as determined from its observation as a product of the reaction between [U-^{13}C]ribose and PLL

The assignment of C_5 was aided by the detection of norfuraneol as a product of reaction between ribose and spermidine, where its NMR signal did not overlap with others.

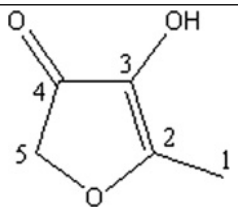

Carbon *n* atom	δ (ppm)	Multiplicity	*J* (Hz)
1	15.9	D	49
2	183.5	Ddd	88, 49, 14
3	136.1	Dddd	88, 65, 20, 3
4	201.5	Ddd	65, 43, 14
5	76.5	Dd	43, 20

© 2014 The Author(s) This is an Open Access article distributed under the terms of the Creative Commons Attribution Licence (CC-BY) (http://creativecommons.org/licenses/by/3.0/) which permits unrestricted use, distribution and reproduction in any medium, provided the original work is properly cited.

REFERENCES

1 Wells-Knecht, K. J., Brinkmann, E., WellsKnecht, M. C., Litchfield, J. E., Ahmed, M. U., Reddy, S., Zyzak, D. V., Thorpe, S. R. and Baynes, J. W. (1996) New biomarkers of Maillard reaction damage to proteins. Nephrol. Dialy Transplant. **11 (Suppl. 5)**, 41–47

2 Biemel, K. M., Reihl, O., Conrad, J. and Lederer, M. O. (2001) Formation pathways for lysine-arginine cross-links derived from hexoses and pentoses by Maillard processes-unraveling the structure of a pentosidine precursor. J. Biol. Chem. **276**, 23405–23412

3 Dunn, J. A., Patrick, J. S., Thorpe, S. R. and Baynes, J. W. (1989) Oxidation of glycated proteins – age-dependent accumulation of N-epsilon-(carboxymethyl)lysine in lens proteins. Biochemistry **28**, 9464–9468

4 Monnier, V. M., Mustata, G. T., Biemel, K. L., Reihl, O., Lederer, M. O., Dai, Z. Y. and Sell, D. R. (2005) Cross-linking of the extracellular matrix by the Maillard reaction in aging and diabetes-an update on “a puzzle nearing resolution”. Ann. N. Y. Acad. Sci. **1043**, 533–544

5 Munanairi, A., O’Banion, S. K., Gamble, R., Breuer, E., Harris, A. W. and Sandwick, R. K. (2007) The multiple Maillard reactions of ribose and deoxyribose sugars and sugar phosphates. Carbohydr. Res. **342**, 2575–2592

6 Biemel, K. M., Friedl, D. A. and Lederer, M. O. (2002) Identification and quantification of major Maillard cross-links in human serum albumin and lens protein-evidence for glucosepane as the dominant compound. J. Biol. Chem. **277**, 24907–24915

7 Hodge, J. E. (1953) Dehydrated foods: chemistry of browning reactions in model systems. Agricult. Food Chem. **1**, 928–943

8 Biemel, K. M., Conrad, J. and Lederer, M. O. (2002) Unexpected carbonyl mobility in aminoketoses: the key to major Maillard crosslinks. Angew. Chemie. Int. Ed. Eng. **41**, 801–803

9 Hauck, T., Hubner, Y., Bruhlmann, F. and Schwab, W. (2003) Alternative pathway for the formation of 4,5-dihydroxy-2,3-pentanedione, the proposed precursor of 4-hydroxy-5-methyl-3(2H)-furanone as well as autoinducer-2, and its detection as natural constituent of tomato fruit. Biochim. Biophys. Acta-Gen. Subj. **1623**, 109–119

10 Ferreira, A. E. N., Freire, A. M. J. P. and Voit, E. O. (2003) A quantitative model of the generation of N-epsilon-(carboxymethyl)lysine in the Maillard reaction between collagen and glucose. Biochem. J. **376**, 109–121

11 Wells-Knecht, M. C., Thorpe, S. R. and Baynes, J. W. (1995) Pathways of formation of glycoxidation products during glycation of collagen. Biochem. **34**, 15134–15141

12 Chuyen, N. V., Kurata, T. and Fujimaki, M. (1973) Formation of N-carboxymethyl amino-acid from reaction of alpha-amino-acid with glyoxal. Agric. Biol. Chem. **37**, 2209–2210

13 Smuda, M., Voigt, M. and Glomb, M. A. (2010) Degradation of 1-deoxy-D-erythro-hexo-2,3-diulose in the presence of lysine leads to formation of carboxylic acid amides. J. Agric. Food Chem. **58**, 6458–6464

14 Henning, C., Smuda, M., Girndt, M., Ulrich, C. and Glomb, M. A. (2011) Molecular basis of maillard amide-advanced glycation end product (AGE) formation *in vivo*. J. Biol. Chem. **286**, 44350–44356

15 Cistola, D. P., Small, D. M. and Hamilton, J. A. (1982) Ionization behavior of queous Short-Chain Carboxylic-Acids-a C-13 NMR-Study. J. Lipid Res. **23**, 795–799

16 Hagen, R. and Roberts, J. D. (1969) Nuclear magnetic resonance spectroscopy. 13C spectra of aliphatic carboxylic acids and carboxylate anions. J. Am. Chem. Soc. **91**, 4504–4506

17 Zou, J., Guo, Z. J., Parkinson, J. A., Chen, Y. and Sadler, P. J. (1999) Gold(III)-induced oxidation of glycine. Chem. Commun. 1359–1360

18 Kalinowski, H.-O., Berger, S. and Braun, S. (1988) Carbon 13 NMR Spectroscopy, Wiley

Received 11 December 2013/15 January 2014; accepted 29 January 2014

Published as Immediate Publication 12 February 2014, doi 10.1042/BSR20130135

© 2014 The Author(s) This is an Open Access article distributed under the terms of the Creative Commons Attribution Licence (CC-BY) (http://creativecommons.org/licenses/by/3.0/) which permits unrestricted use, distribution and reproduction in any medium, provided the original work is properly cited.